

# MMA Memo 221: Elevation Dependence in Fast Switching

M.A. Holdaway  
National Radio Astronomy Observatory  
949 N. Cherry Ave.  
Tucson, AZ 85721-0655  
email: mholdawa@nrao.edu

July 13, 1998

## Abstract

We investigate the dependence of fast switching phase calibration on elevation angle. We include elevation effects such as air mass, change in rms phase, change in the distance between the lines of sight, and the details of the antenna's proposed AZ-EL drive system which is singular at the zenith. We find that the AZ-EL drive system creates a noticeable, but small effect, making very high elevation observations (ie, 75-85 degrees elevation) slightly less sensitive than at the optimum elevation around 70 degrees. The overall elevation behavior is dominated by the increase in rms phase with decreasing elevation. A sensitivity analysis indicates that something like 20 degree residual phase errors will be optimal for high elevations, while 25 or 30 degree residual phase errors will be optimal for low elevations or the highest observing frequencies. We achieve sensitivities of about 80% of the "perfectly phase stable" atmospheric case (which would not require any phase calibration) when we including both the effects of time lost to fast switching calibration and the decorrelation losses due to the residual phase errors inherent in the fast switching phase calibration technique.

## 1 Introduction

The fast switching phase calibration method has been well studied from a theoretical point of view (Holdaway 1992; Holdaway *et al.* 1995; Holdaway, 1997) and from a practical, experimental point of view (Holdaway and Owen, 1995; Carilli and Holdaway, 1997). In fast switching phase calibration, the residual phase errors are given by the square root of the phase structure function  $D_\phi$  evaluated at some effective calibration baseline:

$$\sigma_\phi \simeq \sqrt{D_\phi(v_{atmos}t_{cycle}/2 + d)}, \quad (1)$$

where  $t_{cycle}$  is the full calibration cycle time,  $v_{atmos}$  is the atmospheric velocity aloft, and  $d$  is the distance between the lines of sight to the calibrator and target source at the altitude

of the turbulence. However, one question that has not been explicitly addressed has been the elevation dependence of fast switching’s ability to correct for the atmospheric phase errors. Of primary concern at this moment is the elevation dependence of a purely azimuthal slew: at an elevation angle  $EL$ , an angle  $\theta$  on the sky requires an azimuthal slew of  $\theta / \cos(EL)$ . In addition to the elevation dependent slewing times, we also need to be concerned with the variation of opacity with elevation ( $1 / \sin(EL)$ ), the variation of rms phase with elevation ( $\sqrt{1 / \sin(EL)}$ ), and the variation of the distance  $d$  between the lines of sight ( $1 / \sin(EL)$ ). These effects cannot be folded into an estimate of the phase stability analytically, but numerical simulations can handle everything.

## 2 Simulation Details and Assumptions

In order to perform realistic simulations of fast switching, we need to have somewhat realistic models of several aspects of the array’s environment, capabilities and operation:

- **sensitivity:** we assume an array of 36 10 m antennas, 25 micron surfaces with Ruze law degradation, and 85% efficiency at the low frequency limit. We assume that the system temperatures at the various target frequencies are those given in MMA Memo 201 (Holdaway, 1998), and that the opacity varies with frequency on the Chajnantor site as measured experimentally by Matsuo *et al.*.
- **antenna slewing:** as per the suggestions of the antenna working group, the maximum slew rates and accelerations are 3 deg/s and 12 deg/s/s for the elevation drive and 6 deg/s and 24 deg/s/s in the azimuth drive. We utilize Gaussian velocity slewing profiles (see Appendix A for a detailed discussion).
- **set up times:** earlier fast switching calculations for the MMA had used various “settle down” or “setup” times. As the slewing profiles used do not excite the antenna’s lowest resonant frequency, there is no settle down time. Further, we assume that the on-line system setup is concurrent with slewing (ie, the on-line system is able to switch sources in about 1 s or less, the typical slew time).
- **opacity:** the 225 GHz opacities were taken over the year between May 1995 and April 1996. The empirical relationships of Matsuo *et al.* are used to scale the 225 GHz opacities to opacities at other frequencies.
- **phase stability:** the 11.2 GHz phase monitor data were taken over the year between May 1995 and April 1996. The root structure function power law exponent depends upon the phase conditions, and ranges from 0.54 during the best condition bin to 0.64 for the worst condition bin.
- **phase stability with elevation:** we assume that the phase structure function on short baselines (ie, the effective calibration baselines of 30-300 m used in fast switching ob-

servations) increases proportionally to the air mass, or that the rms phase varies as the square root of the airmass (Holdaway and Ishiguro, 1995).

- **atmospheric velocity:** we used 12 m/s, close to the median value of the winds aloft determined from the interferometer data.
- **scheduling strategy:** we use the same scheduling strategy as used in MMA Memo 174 (Holdaway, 1997): the highest frequency observations are given the best *phase stability* conditions, and so on, with an assumed distribution of the demand for observations of various frequencies ranging from 40 to 650 GHz. Since opacity and phase stability are not perfectly correlated, the lowest opacity conditions are not necessarily chosen for the highest frequency observations.

As we treat observations over a range of elevation angles (from 30 deg to 85 deg) in the present work, we assume that all elevations at a given frequency are observed during the same phase stability conditions. This is suboptimal as the low elevation observations will actually require significantly better phase stability than the high elevation observations.

- **fast switching strategy:** we calibrate at 90 GHz for all observations. For higher target frequencies, we will need to get extra SNR on the calibrator source to permit extrapolation of the calibrator phase to the target source’s frequency.
- **simulated calibrator fields:** sample fields of potential calibrator sources consistent with the source counts of Holdaway, Owen, and Rupen (1994, MMA Memo 123). For each bin of atmospheric conditions (phase stability and opacity) observations of a single frequency and of elevation angles of 30, 60, 70, 75, 80, and 85 degrees were each given 200 simulated calibrator fields. The calibrator with the optimal  $vt/2 + d$  for that frequency and elevation was chosen considering the slew time to get to the source (correctly treating AZ and EL drive velocities), the time required to detect the calibrator with ample SNR, including opacity contributions to the sensitivity, and including the dependence of  $d$ , the distance between the lines of site to calibrator and target source, with elevation.

### 3 Evaluating the Results

We start with a pretty but misleading illustration. What if we were to adopt the same fast switching observing strategy at each elevation, spending, say, only 50% of the cycle time on the target source: how would things change with elevation? We answer that question in Figure 1. While this graph is somewhat misleading (this is not the strategy one would employ for observing at the different elevations), it illustrates the different elevation effects. The open boxes represent  $vt/2 + d$  as a function of elevation, not including the increase in rms phase with airmass. At high elevations, the extra slew time required to reach a suitable calibrator due to the azimuthal singularity at the zenith can clearly be seen. At low elevations, the increased opacity and the increased  $d$  term between the lines of sight increase the  $vt/2 + d$  modestly. The solid boxes attempt to approximate the effect of the atmospheric phase errors increasing as the

square root of the air mass (which is equivalent to increasing the effective calibration baseline by the air mass). The most striking feature of the data points is the increase in effective  $vt/2 + d$  at low elevations.

Now, this is not exactly what we would do if we were observing with the MMA. Instead of spending 50% of the time on the target source, we might actually spend a much larger fraction of the time on the target source at the high elevations where the  $vt/2 + d$  is low, and a smaller fraction of the time on the target source for the low elevations. We can turn the problem around and ask what the cycle time should be such that our residual phase errors on each baseline are less than some amount, say 25 deg. This way of looking at the problem is demonstrated in Figure 2. For the 345 GHz bin of conditions, we show how fast the cycle time will need to be to obtain 25 deg. In addition, we also indicate the contribution to the cycle time due to slewing and integrating on the calibrator source. The rest of the time is spent integrating on the target source, since we have assumed no setup time in addition to the slew time. It is also easy to determine the fraction of time the target source is observed. As can be seen, the fraction of time spent on source is low at low elevations where the cycle time must be very short to keep up with the atmosphere, and also a bit low at high elevations where the time spent slewing to and from the calibrator is larger due to approaching the zenith singularity for an AZ-EP drive system. However, because the cycle time required to achieve the desired residual phase error at high elevation is quite large, and because the fast switching overhead is a rather modest fraction of the entire cycle time, observations at high elevation angle are not adversely affected by the zenith singularity.

We can take this analysis a bit further. We want the residual phase errors to be as small as possible, but to get them very small may actually require that we spend a very small fraction of our cycle time integrating on the target source. The tradeoffs are very straightforward: we will usually wish to optimize the array's sensitivity. The residual phase errors will result in sensitivity loss via decorrelation as

$$e^{-\sigma_\phi^2/2}, \quad (2)$$

and the lost time spent on fast switching will result in sensitivity loss as

$$\sqrt{t_{target}/t_{cycle}}. \quad (3)$$

As these two factors will push  $t_{cycle}$  in opposite directions, there will be a  $t_{cycle}$  (and hence, a residual phase error level) which results in the optimal sensitivity for each observing frequency and elevation. Figure 3 shows plots of the sensitivity curves for 20, 25, and 30 degree residual phase errors (including a 10 degree rms in the calibrator gain solutions due to thermal noise; since the time spent integrating on the calibrator is usually very small, not much can be gained in  $vt/2 + d$  by relaxing the rms in the gain solutions). At high elevations and at low frequencies, the 20 degree residual phase errors result in near optimal sensitivity. At the higher frequencies and at lower elevation angles, it is not always possible to achieve 20 degree residual phase errors as the required cycle time to do so may be less than the slew time and calibrator integration time. Hence, the sensitivity of high frequency and low elevation observations is optimized by larger residual fast switching phase errors.

Elevation Dependence in Fast Switching at 345 GHz

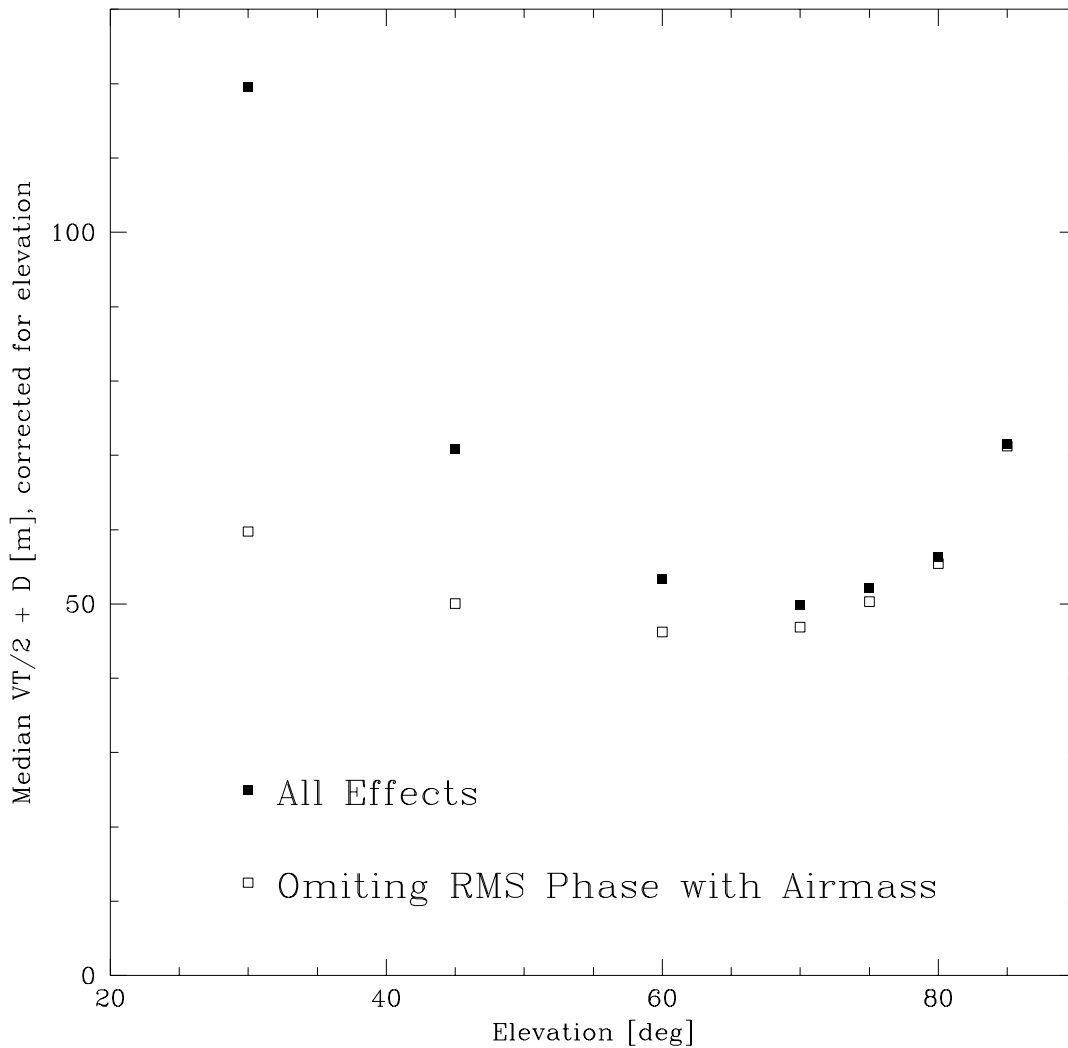


Figure 1:  $vt/2 + d$  as a function of elevation for 345 GHz observations, spending 50% of the time on the target source. The open boxes represent the values of  $vt/2 + d$  which result from including all elevation dependent effects except for the increase in rms phase with increasing air mass. The solid boxes attempt to approximate the effect of the atmospheric phase errors increasing as the square root of the air mass (which is equivalent to increasing the effective calibration baseline by the air mass). A much more dramatic increase in  $vt/2 + d$  is seen at low elevations.

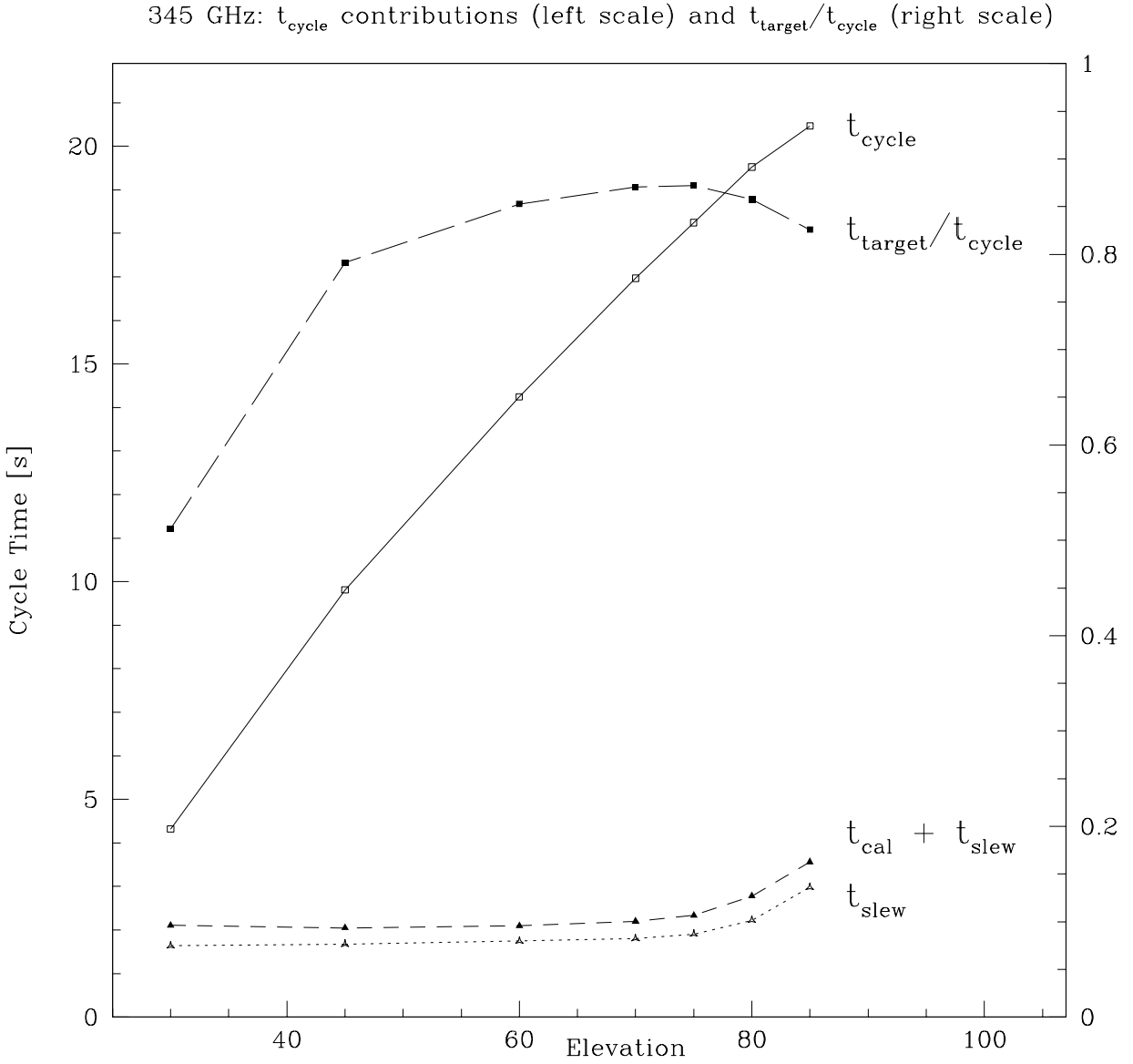


Figure 2: The  $t_{\text{cycle}}$  required for 345 GHz observations to have  $25^\circ$  rms residual phase errors, as a function of elevation. Contributions to  $t_{\text{cycle}}$  include the two way slew time, the calibrator integration time, and the integration time on the target source. Also graphed is the on-source fraction,  $t_{\text{target}}/t_{\text{cycle}}$ .

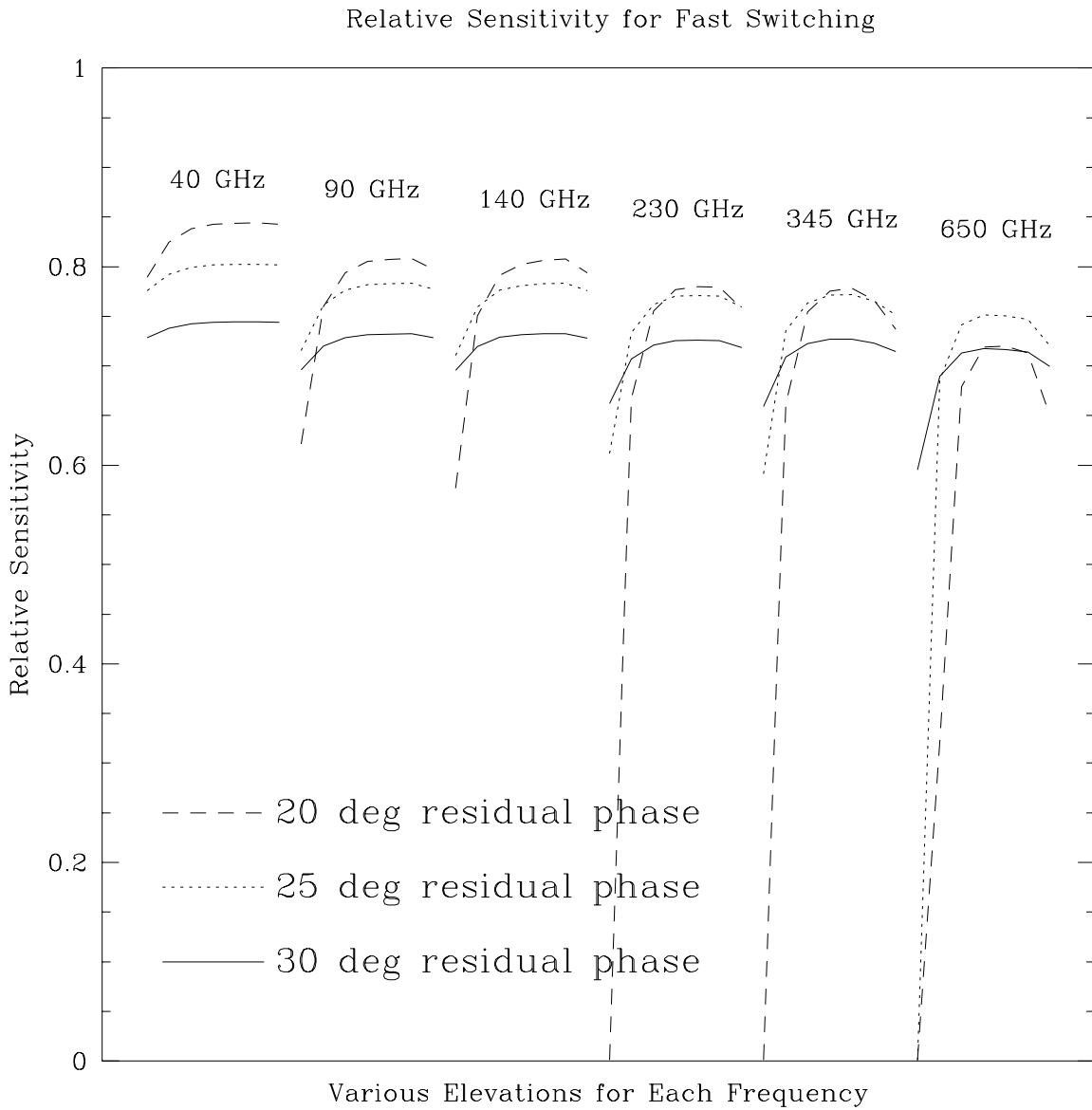


Figure 3: Relative sensitivity due to fast switching effects as a function of elevation for several different frequencies. Sensitivity loss due to time spent off-source during fast switching and due to decorrelation from the residual phase errors are included. The left side of each single frequency curve is at the low elevation of  $30^\circ$ , and the right side of each curve is at  $85^\circ$ .

## 4 Conclusions

We find that the performance of fast switching at high elevation angles (ie, above 70 degrees) is not adversely affected by the zenith singularity in the AZ-EL drive system. However, fast switching, or any other phase correction scheme for that matter, will have an increasingly difficult job at removing the phase fluctuations at low elevations, say below 30 degrees.

## A Antenna Slewing Details

As pointed out by David Woody (unpublished communication), the fast switching antenna motion profile can be chosen such that the excitation of the antenna's lowest resonant frequency (LRF) is insubstantial. One such velocity profile, based on a suggestion by David Woody, is a simple Gaussian with time:

$$v(t) = v_o e^{-(t/t_o)^2}, \quad (4)$$

where  $v_o$  is the maximum velocity and  $t_o$  is the time scale of the slew. The acceleration profile is obtained by differentiation:

$$a(t) = \frac{-2v_o}{t_o^2} t e^{-(t/t_o)^2}, \quad (5)$$

and the position profile is given by integrating the Gaussian velocity profile, which gives the so-called error function. The power spectrum is obtained by Fourier transforming the acceleration profile and squaring it. We are interested in the power injected into the antenna at 6 Hz, a conservative estimate for the LRF. We can decrease the power at the LRF by increasing  $t_o$ , or less effectively by decreasing  $v_o$ . The maximum acceleration is about  $0.86v_o/t_o$  deg/s<sup>2</sup>. The position profile is given by integrating the Gaussian velocity profile, which is the so-called error function.

So, in picking an antenna slewing profile for a particular move, we would like to make the move as short as possible subject to the maximum slewing velocity and acceleration constraints, and also subject to the constraint that we not excite the LRF above some minimum level. I think that without a detailed dynamical understanding of the antenna, we cannot say a priori how much power at the LRF we can tolerate. Fortunately, a small increase in  $t_o$  will result in a very large decrease in the exciting power at the LRF, so a small but arbitrary power level at the LRF will result in  $v_o$  and  $t_o$  which would be similar to the results of a more detailed analysis. In our analysis, we have chosen the maximum allowed power at the LRF to be  $10^{-8}$  of the peak power for a move with  $t_o = 0.2$  s and  $v_o = 3$  deg/s. A much less conservative figure would reduce  $t_o$  only marginally.

Once  $t_o$  and  $v_o$  have been specified, the distance of the slew and the slewing time required are determined. Since the error function position profile asymptotically approaches the starting and stopping positions, we consider the fast switching pointing specification of 3 arcsec to cut off the function at a finite time. As an example, with  $t_o = 0.21$  s and  $v_o = 3.0$  deg/s, the maximum acceleration is 12.0 deg/s/s, the power at the LRF is below our threshold, and a slew of 1.14 deg is achieved in 0.96 s. To make larger slews,  $t_o$  is increased (we would have



liked to increase the velocity, but we are at the maximum, at least for the elevation axis.) To make shorter slews,  $v_o$  is decreased, permitting slight decreases in  $t_o$  (we would have liked to accomplish the shorter slew solely by decreasing  $t_o$ , but this would put too much power at the LRF). Apparently, the maximum velocity and acceleration for the elevation drive are well matched to a 1 degree move in 1 s. By finding the optimal  $t_o$  and  $v_o$  for several different length moves, we are able to generate a lookup table for both elevation and azimuth drives. In the Monte Carlo simulations of the calibrator fields, we use interpolated slew times from this table to determine the optimal calibrator to use for a given simulated observation.

### References

Carilli, C.L, Holdaway, M.A., 1997, "Application of Fast Switching Phase Calibration at mm Wavelengths on 33 km Baselines", MMA Memo 173.

Holdaway, M.A., 1992, "Possible Phase Calibration Schemes for the MMA", MMA Memo 84.

Holdaway, M.A., 1997, "How Many Fast Switching Cycles Will the MMA Make in its Lifetime?", MMA Memo 174.

Holdaway, M.A., 1998, "Hour Angle Ranges for Configuration Optimization", MMA Memo 201.

Holdaway, M.A., and Ishiguro, Masato., 1995, "Experimental Determination of the Dependence of Tropospheric Pathlength Variation on Airmass", MMA Memo 127.

Holdaway, M.A., Owen, F.N., and Rupen, M.P., 1994, "Source Counts at 90 GHz", MMA Memo 123.

Holdaway, M.A., Owen, F.N., 1995, "A Test of Fast Switching Phase Calibration with the VLA at 22GHz", MMA Memo 126.

Holdaway, M.A., Simon J.E. Radford, F.N. Owen, Scott M. Foster, 1995 "Fast Switching Phase Calibration: Effectiveness at Mauna Kea and Chajnantor", MMA Memo 139.

Matsuo, Hiroshi; Sakamoto, Akihiro; and Matsushita, Satoki, 1998, "FTS measurements of submillimeter-wave opacity at Pampa la Bola", submitted to PASJ.